

Metastable resistivity of $\text{La}_{0.8}\text{Ca}_{0.2}\text{MnO}_3$ manganite thin films

V. Markovich,¹ G. Jung,¹ Y. Yuzhelevskii,¹ G. Gorodetsky,¹ F. X. Hu,² and J. Gao²

¹*Department of Physics, Ben-Gurion University of the Negev, P.O. Box 653, 84105 Beer-Sheva, Israel*

²*Department of Physics, The University of Hong Kong, Pokfulam Road, Hong Kong, China*

(Received 1 November 2006; revised manuscript received 11 January 2007; published 23 March 2007)

Transport properties of $\text{La}_{0.8}\text{Ca}_{0.2}\text{MnO}_3$ thin films 15 and 130 nm thick have been investigated and confronted with the properties of bulk single crystals of the same composition. It has been found that low-temperature resistivity of the films is sensitive to electric current and/or field treatment and thermal history of the sample. Thin films exhibit a variety of metastable resistive states and spontaneously evolve toward high-resistivity state in which the films exhibit highly nonlinear transport behavior at low temperatures. Nonlinear V - I characteristics are well described by indirect tunneling model. The memory of the resistivity can be, at least partly, erased by a heat treatment at temperatures above the memory erasing temperature. The memory erasing temperature for thin films, $T=450$ K, is significantly higher than that of single crystals. The results are interpreted in the context of strain driven phase separation. Coexistence of two ferromagnetic phases with different orbital orders and different conductivities is influenced by strains due to thermal cycling and current flow.

DOI: [10.1103/PhysRevB.75.104419](https://doi.org/10.1103/PhysRevB.75.104419)

PACS number(s): 75.47.Lx, 73.63.-b, 75.47.Gk

I. INTRODUCTION

Physical properties of perovskite transition-metal oxides are determined by mutual cross coupling between spin, charge, and lattice degrees of freedom.^{1,2} The perovskite-manganese oxides $\text{La}_{1-x}\text{Ca}_x\text{MnO}_3$ (LCMO) belong to a group of strongly correlated electron systems exhibiting colossal magnetoresistance (CMR) effect. Metal-insulator transition in LCMO is observed within the doping range $x=0.15$ – 0.5 . Experiments prove that magnetic and transport properties of doped CMR manganites depend not only on the doping level and average radius of A -site cation^{1,2} but also on magnetic,³ electric,^{4,5} and thermal⁶ history of a sample. One of the most characteristic features of doped manganites, which is responsible for their extremely rich phase diagram and may even lie at the core of the very CMR effect, is a dynamic coexistence of phases with different magnetic and electronic properties, known as phase separation (PS).¹ Theoretical models predict appearance of spontaneous PS on nanometer scale and strain induced phase separation on nanometer up to micrometer length scale. Therefore, lattice distortions and long-range strains affect PS in doped manganites.^{1,2,6}

Metastability seems to be a generic feature of phase separated systems with two or more competing ordering mechanisms. Double exchange (DE) interactions establish ferromagnetic (FM) ordering in CMR manganites through a strong Hund's coupling between e_g electrons of neighboring Mn^{3+} and Mn^{4+} sites. In LCMO manganites doped slightly below the percolation threshold $x_C=0.225$, an insulating FM phase incompatible with DE mechanism has been observed. It turns out that superexchange interactions and orbital ordering (OO) govern transport and magnetic properties of lowly doped manganites hand in hand with DE interactions.⁷⁻⁹

Thin films of doped manganites exhibit several unusual features, such as nonlinear conductivity, strain induced hysteretic behavior, appearance of metastable resistivity, slow response of the resistance to external stimuli, and memory effects.¹⁰⁻¹⁵ Recently, a pronounced glassy behavior of the

resistance was observed in very thin $\text{La}_{0.8}\text{Ca}_{0.2}\text{MnO}_3$ films.¹⁴ It was found that applied magnetic and gated electrostatic fields increase the volume occupied by one of the coexisting phases. The resulting resistance changes were associated with the motion of boundaries between coexisting phases. Similar phenomena were observed by us in LCMO bulk manganite single crystals doped at $x=0.18$ and 0.2 .^{4,5}

It is well known that strain in manganite films increases with decreasing thickness of the film. Increased strain levels lead to more pronounced phase separation, influencing many physical properties of the system. For example, PS state of thin $\text{La}_{0.67}\text{Ca}_{0.33}\text{MnO}_3$ films, which was shown to be strain driven,¹¹ is composed of metallic and charge-ordered insulating FM regions, which are completely esoteric for this composition and never appear in the bulk.

Shreekala *et al.*¹⁶ have shown that the unit cell volume of $\text{La}_{0.8}\text{Ca}_{0.2}\text{MnO}_3$ thin film is much smaller than that of the bulk, resulting in an enhancement of the transfer integral of electron hopping and corresponding increase of e_g electron bandwidth. Consequently, both the metal-insulator transition and Curie temperature increase. This remains in agreement with the results of studies of magnetic and transport properties of lowly doped LCMO crystals under pressure, which show that hydrostatic pressure increases T_C and decreases the resistivity at all temperatures.⁹

In this paper, we discuss transport properties of very thin ($d\sim 15$ nm) and moderately thin ($d\sim 130$ nm) epitaxial $\text{La}_{0.8}\text{Ca}_{0.2}\text{MnO}_3$ films with different strain levels and compare them with the properties of bulk single crystals. The research was triggered by a recent report on current induced metastable states and strong effects of dc on electric resistivity in very thin $\text{La}_{0.8}\text{Ca}_{0.2}\text{MnO}_3$ films.¹⁵

II. EXPERIMENTAL AND RESULTS

The studied $\text{La}_{0.8}\text{Ca}_{0.2}\text{MnO}_3$ thin films were fabricated on (100) oriented SrTiO_3 substrates by means of off-axis rf-magnetron sputtering technique.¹⁷ Sintered stoichiometric disks of $\text{La}_{0.8}\text{Ca}_{0.2}\text{MnO}_3$ with diameter of 50 mm and thick-

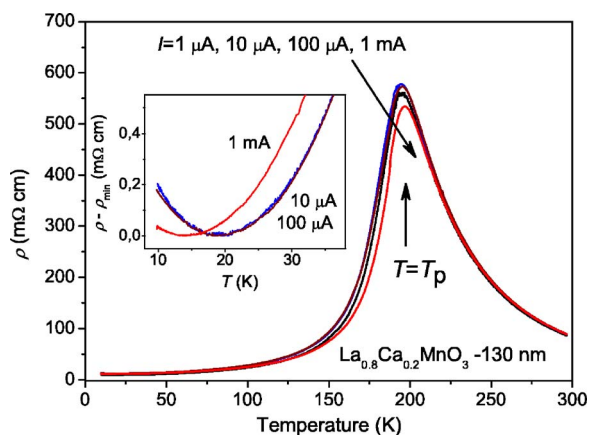


FIG. 1. (Color online) Temperature dependence of the resistivity of $\text{La}_{0.8}\text{Ca}_{0.2}\text{MnO}_3$ 130 nm film in the pristine state recorded during cooling at various currents. The inset shows the variation of the resistivity in the vicinity of low-temperature minimum. ρ_{\min} is the resistivity of the film at $T_{\min} \approx 19.5$ K.

ness of ~ 4 mm were used as sputtering targets. Sputtering was performed at rf power density of 3.7 W/cm^2 in argon and oxygen mixture with a ratio of $\text{Ar}:\text{O}_2 = 1:2$ at a pressure of 1.5×10^{-1} mbar. The predeposition background pressure in the sputtering chamber was lower than 5×10^{-6} mbar. The substrate was mounted directly on the heater by means of silver paste. The substrate temperature during deposition was kept at 730°C . The thickness of the films was controlled by the deposition time. After the deposition, the films were annealed at 800°C in air for 30 min. The x-ray diffraction patterns proved that the films are highly epitaxial and of a single phase. The out-of-plane lattice parameter of a thinner film is smaller than that of a thicker one, indicating that the tensile strain is stronger in thinner film.

Curie temperature T_C determined from the magnetization measurements in magnetic field of 100 Oe was 235 K for thinner and 200 K for thicker films. Both temperatures are much higher than T_C of 184 K in bulk $\text{La}_{0.8}\text{Ca}_{0.2}\text{MnO}_3$ single crystals.⁹

Measurements of voltage-current characteristics (V - I) and of differential resistance ($R_d = dV/dI$) were performed in a standard four-point arrangement. The separation between voltage probes was 0.4–0.5 mm. To avoid excessive Joule heating, the measuring dc was periodically turned on and off during data recording at each temperature. Dynamic resistance was measured directly with a phase-sensitive lock-in detector using $5 \mu\text{A}$ ac modulation at 390 Hz.

The results show significant differences between temperature evolution of the resistivity of thicker and thinner films and single crystals of the same composition. Resistivity of a thicker film recorded during slow cooling under various dc bias currents is shown in Fig. 1. One can see clear metal-to-insulator transition (MIT) at $T_p \approx 195$ K and metalliclike behavior below T_p . No significant thermal hysteresis has been seen in the measurements. The $\rho(T)$ curves recorded at heating and cooling cycles with bias currents in the 1–100 μA range practically coincide. The small (5%) reduction of the resistivity in the vicinity of T_p in $\rho(T)$ curve recorded at $I = 1$ mA is likely related to anomalous thermal effects due to

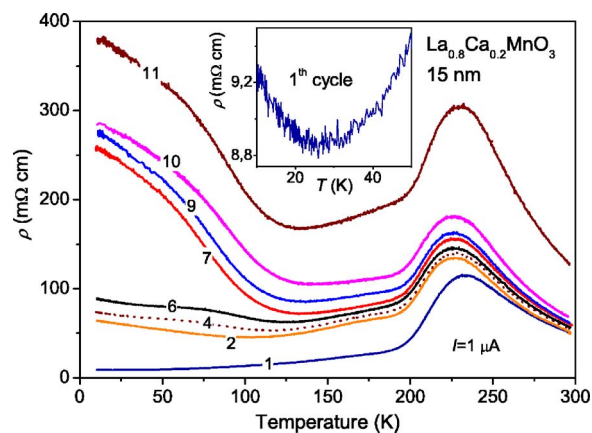


FIG. 2. (Color online) Evolution of the temperature dependence of resistance of $\text{La}_{0.8}\text{Ca}_{0.2}\text{MnO}_3$ 15 nm film during progressive thermal cycling. Curves are labeled with the numbers of preceding thermal cycles.

small heating and cooling steps related to turning on and off the dc, as discussed recently in Ref. 18.

Thicker film in the pristine state exhibits well defined resistivity minimum at $T_{\min} \approx 19.5$ K, shown in the inset of Fig. 1. A shift of the position of the minimum to 14 K under applied current of 1 mA may be attributed to possible heating effect, consistent with the fact that the resistivities recorded at lower currents, between 10 and 100 μA , practically coincide. The appearance of such low-temperature resistivity minimum is interpreted in the literature as being due to quantum corrections to low-temperature conductivity in the presence of disorder.^{19,20}

The resistivity of single crystals and thicker films is practically stable with respect to thermal cycling.⁵ In a marked contrast, the resistivity of very thin films changes after each cycle of cooling down to 10 K and reheating back to room temperatures. A set of $\rho(T)$ of $\text{La}_{0.8}\text{Ca}_{0.2}\text{MnO}_3$ thinner film (15 nm) recorded during subsequent cooling cycles is shown in Fig. 2. The resistivity progressively increases with thermal cycling in the entire experimental temperature range. The effect is most pronounced at low temperatures below $T \sim 100$ K, where the character of resistivity changes from metallic to semiconductinglike one. Additionally, thinner films also exhibit well defined resistivity minimum at $T_{\min} \approx 26$ K (see inset of Fig. 2).

For a detailed discussion of the resistive properties of $\text{La}_{0.8}\text{Ca}_{0.2}\text{MnO}_3$ single crystals, the reader is referred to our previous papers.⁵ Let us remind here briefly that the bulk crystal resistivity in the pristine state, see inset of Fig. 3, exhibits a pronounced maximum at $T \approx T_C = 184$ K, followed by a minimum around 140 K, subsequent upturn toward a broad maximum at $T \sim 70$ K, and a final decrease to the low-temperature constant value.

Although $\rho(T)$ curves of bulk crystals and thinner and thicker film samples look markedly different, the basic character of the mechanisms responsible for the resistivity seems to be the same. The high-temperature paramagnetic part of all $\rho(T)$ curves can be well approximated by a thermally activated process with a single activation energy,

$$\rho(T) = \rho_{\infty} \exp(E_d/k_B T). \quad (1)$$

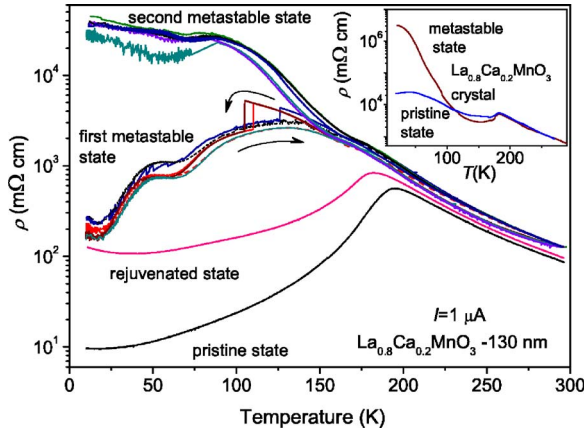


FIG. 3. (Color online) Thermal dependence of the resistance of $\text{La}_{0.8}\text{Ca}_{0.2}\text{MnO}_3$ 130 nm film in distinct metastable states confronted with the resistance in the pristine and rejuvenated states. Inset: Resistance of the bulk $\text{La}_{0.8}\text{Ca}_{0.2}\text{MnO}_3$ single crystal in pristine and high-resistivity metastable state.

Performing the fit for thicker films in the temperature range $210 \text{ K} \leq T \leq 295 \text{ K}$, we obtain $E_a = 100 \pm 10 \text{ meV}$. Activation energies obtained in the same temperature range for pristine state thinner films and bulk $\text{La}_{0.8}\text{Ca}_{0.2}\text{MnO}_3$ crystals are $E_a = 95 \pm 10 \text{ meV}$. These values are consistent with the activation energies reported in the literature for various bulk and thin-film manganite samples.^{21–23}

In general, the $\text{La}_{0.8}\text{Ca}_{0.2}\text{MnO}_3$ samples' resistivities are not compatible with metallic transport. Nevertheless, in a limited temperature range below T_C , one can consider the system to behave like a metallic one in the sense of $dR/dT > 0$. It has been demonstrated by a recent comprehensive study of various $\text{La}_{0.7}\text{A}_{0.3}\text{MnO}_3$ ($A = \text{Ca}, \text{Sr}$) thin films grown by different techniques on several substrates that the low-temperature part of the $\rho(T)$ dependence exhibiting metalli-like resistivity can be well fitted by a simple power function,²²

$$\rho(T) = \rho_0 + AT^\alpha. \quad (2)$$

The exponent $\alpha = 2$ is a hallmark of the domination of electron-electron scattering and deviations from the quadratic power law can be attributed to contributions of other scattering mechanisms.²²

We have fitted experimental dependences of the resistivity in the temperature range between T_{\min} and T_i , where $T_i = 60, 70, 80, \dots, 130 \text{ K}$ and found that Eq. (2) approximates well our experimental data. For thicker films, the parameter α varies between 2.9 and 3.1, depending on the temperature range. The resistivity of thinner films in the pristine state, curve 1 in Fig. 2, can also be fitted to Eq. (2) with $\alpha \approx 2.4$ for all temperature ranges. It has been shown recently that α increases with increasing residual resistivity and approaches 3 for ρ_0 exceeding $2 \text{ m}\Omega \text{ cm}$.²² The residual resistivity obtained by us from the fitting procedures is well above this threshold value. The ρ_0 of thinner films is $9 \text{ m}\Omega \text{ cm}$, while that of thicker films is $8 \text{ m}\Omega \text{ cm}$. Let us remind that α approaching 3 can be seen as a signature of

unconventional one-magnon scattering, which becomes dominant at high disorder level, and associated reduction of the effective bandwidth of charge carriers.²⁴

During initial measurements of current dependence of R_d for thicker films, we did not observe any transitions to metastable resistive states. Nevertheless, after several thermal cycles, the sample has spontaneously switched to two subsequent metastable states characterized by different resistivities with different temperature evolutions. As illustrated in Fig. 3, the differences became pronounced only at low temperatures below the MIT point. While cooling the sample in the first metastable state, the resistivity continues to increase even for temperatures lower than T_C . Then, at a certain temperature between 100 and 120 K, the resistivity abruptly jumps down. The jump seen in the first cooling cycles is very sharp and occurs in the temperature range below 150 K. The temperature of the jump shifts to lower temperatures with increasing number of thermal cycles. The abrupt jump, which is not seen in the heating cycles, causes a pronounced thermal hysteresis of the resistivity, a feature totally absent in the pristine state. Yet another aspect of the metastable state is the appearance of $\rho(T)$ plateau between 50 and 70 K. The plateau is observed in both cooling and heating cycles.

As a result of application of several current ramping during $V-I$ measurements, the thicker film spontaneously transitioned to yet another metastable resistivity state, which will be referred to as the second metastable state. In this state, the resistivity continuously increases with decreasing temperature, without jumping down as it was in the first metastable state. At lower temperatures, the increase rate slows down and a resistivity plateau appears at intermediate temperatures around 100 K. Thermal hysteresis is practically absent in the second metastable state.

The metastability of thicker films resembles closely the properties of $\text{La}_{0.8}\text{Ca}_{0.2}\text{MnO}_3$ bulk single crystals. The bulk resistivity was found to spontaneously transit to higher resistivity metastable state during a prolonged sample permanence at low temperatures.⁵ The probability of such transition is strongly enhanced by ramping bias current and/or magnetic field, as well as by increasing number of thermal cycles. Similar to the behavior of thin films, the resistivity of $\text{La}_{0.8}\text{Ca}_{0.2}\text{MnO}_3$ crystal in freshly established metastable resistivity state exhibits jumps and jiggles in $R(T)$, which becomes relatively stable only after a few subsequent thermal cycles.

One of the puzzling characteristics of the metastable resistivity in bulk single crystals is a possibility of erasing freshly created metastable states by heat treatment in air at temperatures above 360 K. We have found that heat treatment at temperatures somewhat higher ($\sim 450 \text{ K}$) than those employed in the single-crystal case may also rejuvenate pristine resistivity state in thicker films. Nothing conclusive can be said about rejuvenating the pristine state in thinner films since contacts to 15-nm-thick samples always became non-linear and unfit for measurements after the thermal treatment.

The $\rho(T)$ characteristics of pristine and rejuvenated state are plotted along the metastable $\rho(T)$ in Fig. 3. Note that the rejuvenated state exhibits MIT transition at $T_p \approx 183 \text{ K}$ followed by a metalliclike behavior below T_p and low-

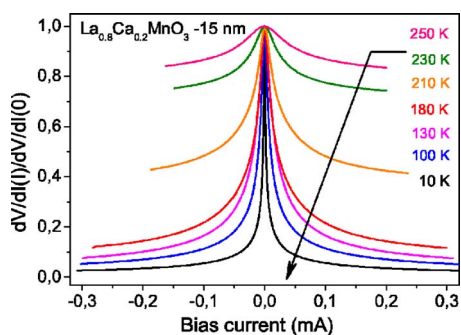


FIG. 4. (Color online) The normalized dynamic resistance of $\text{La}_{0.8}\text{Ca}_{0.2}\text{MnO}_3$ 15 nm film as a function of current at various temperatures.

temperature upturn below $T_{\text{min}} \approx 40$ K. Although the MIT temperatures of the pristine and rejuvenated states are different and their $\rho(T)$ do not fully coincide at low temperatures, the resistivity in both states is likely governed by a similar scattering mechanism. Fitting of $\rho(T)$ of the rejuvenated state in the paramagnetic temperature range, $210 \text{ K} \leq T \leq 295 \text{ K}$, by Eq. (1) gives $E_a \approx 105$ meV, a value very close to the pristine state activation energy. Equation (2) applied to the metalliclike conductivity in temperature range between 45 and 100, 110, 120, or 130 K approximates well the experimental data but with significantly higher parameter $\rho_0 = 70 \text{ m}\Omega \text{ cm}$. Nevertheless, similar to the pristine state, the parameter α varies between 2.7 and 3.1, depending on the temperature range.

In the paramagnetic temperature range, the V - I characteristics of all samples are almost linear and the effect of current flow on R_d is negligible. Below the MIT point temperature, the V - I characteristics become progressively nonlinear, as illustrated in Figs. 4 and 5 for the case of a thinner film. Note that nonlinear resistivity is frequently observed in phase separated manganite thin films,^{15,25,26} tunnel junctions,²⁷ and single crystal.^{4,28,29} The increasing nonlinearity of V - I curves may be seen as a fingerprint of increasing of the contribution of the tunneling mechanisms to the conductivity with decreasing temperature. In description of

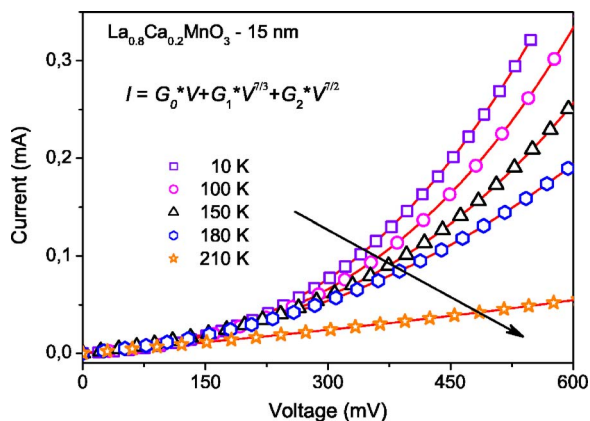


FIG. 5. (Color online) Experimental points of current vs voltage dependences of $\text{La}_{0.8}\text{Ca}_{0.2}\text{MnO}_3$ 15 nm film fitted (solid line) by the GM tunneling theory.

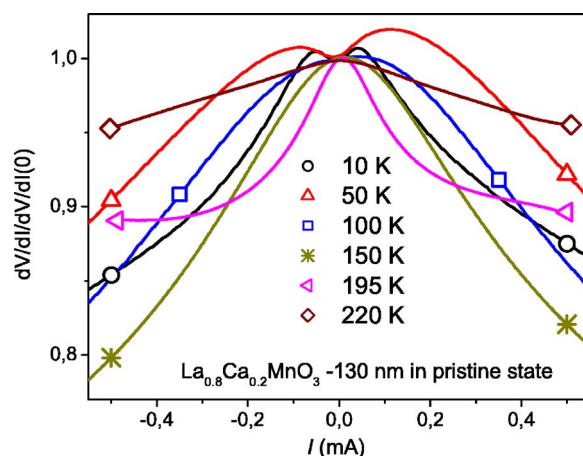


FIG. 6. (Color online) The normalized dynamic resistance $dV/dI(I)/dV/dI(0)$ of 130 nm $\text{La}_{0.8}\text{Ca}_{0.2}\text{MnO}_3$ thin film as a function of bias current at various temperatures.

the tunneling conductivity, we refer to the Glazman-Matveev (GM) model of indirect tunneling.³⁰ The GM theory has been previously employed by us to describe nonlinear V - I characteristics of lowly doped LCMO crystals⁴ and $\text{La}_{0.7}\text{Ca}_{0.3}\text{MnO}_3$ thin films (15 nm).³¹ In the framework of the GM model, the V - I dependence is expressed as multistep tunneling via n localized states. For $eV \gg k_B T$, one has

$$I = (G_0 + G_1)V + \sum_{n=2}^{\infty} a_n V^{n+1-2/(n+1)}, \quad (3)$$

where coefficients a_n are exponential functions of the barrier thickness. Coefficient G_0 accounts for the direct tunneling, G_1 for the resonant tunneling via one impurity, while the nonlinear terms describe inelastic multistep tunneling via localized states. We were able to fit the experimental V - I dependences of thinner films to the GM model using $n=2$ and $n=3$ nonlinear terms only, as shown in Fig. 5. With temperature increasing above 50 K, both nonlinear terms start to decrease while the linear term progressively increases. At temperatures above $T \sim 180$ K, the linear term fully dominates the conductivity and coefficients a_2 and a_3 are practically reduced to zero.

Current dependence of the differential resistance R_d of a thicker film in the pristine state is shown in Fig. 6. The dependence was recorded during the initial thermal cycling which does not influence the resistivity. At high temperatures, V - I curves are almost linear and the differential resistance does not depend on bias. With decreasing temperature, the nonlinearity appears and $R_d(I)$ characteristics start to resemble that of a tunnel junction. In particular, a pronounced zero-bias anomaly (ZBA) appears at temperatures between 10 and 50 K. A similar “abnormal” zero-bias anomaly in the form of a conductivity maximum has been previously observed by us in the low-temperature conductivity of self-doped $\text{La}_{0.89}\text{MnO}_3$ and $\text{La}_{0.82}\text{Ca}_{0.18}\text{MnO}_3$ single crystals.^{4,32} We have attributed the abnormal ZBA to spin-sensitive tunneling through magnetic states located inside barriers of intrinsic tunneling junctions.^{4,32,33} Voltage-current characteris-

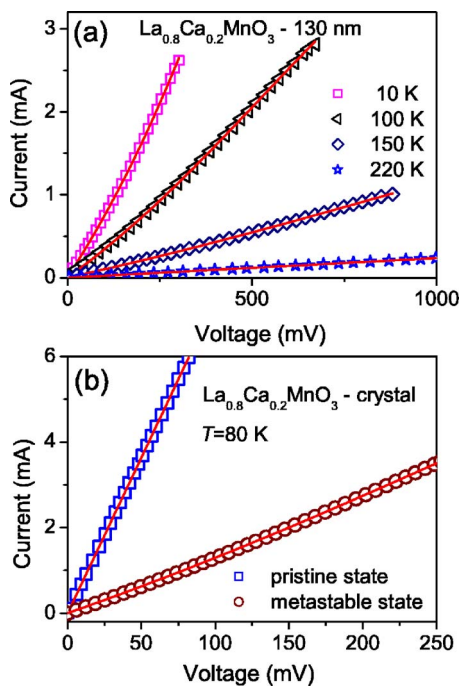


FIG. 7. (Color online) (a) Experimental points of current vs voltage dependences of $\text{La}_{0.8}\text{Ca}_{0.2}\text{MnO}_3$ 130 nm film fitted (solid line) by the multistep tunneling GM theory. (b) Experimental points of current vs voltage dependences of $\text{La}_{0.8}\text{Ca}_{0.2}\text{MnO}_3$ crystal at 80 K in pristine and high-resistivity metastable states fitted (solid line) by the multistep tunneling GM theory.

tics of thicker films in the pristine state are well described by the GM model [see Fig. 7(a)]. The parameters a_2 and a_3 obtained for thicker films are much smaller than those for thinner films. Unfortunately, we were not able to obtain $R_d(I)$ dependencies for the first metastable state in thicker films because during the thermal cycling our samples spontaneously switched to the second metastable resistive state in which the low-temperature resistance exceeded the measuring capabilities of our setup.

Finally, for completeness of the picture, we have also fitted the V - I characteristics of $\text{La}_{0.8}\text{Ca}_{0.2}\text{MnO}_3$ bulk single crystal to the GM model. The characteristics recorded⁵ in the pristine and highly resistive metastable state at $T=80$ K, together with their fit to GM model, are shown in Fig. 7(b). Remarkably, the nonlinearity of V - I characteristics is barely visible even in the metastable state.

III. DISCUSSION

While analyzing current influence of the resistivity, one has to consider first the Joule heating by current flow which may be the real cause of nonlinear V - I characteristics.³⁴⁻³⁷ Current flow which causes a significant heating effect would shift the temperature of the metal-insulator transition to lower temperatures, as was observed in overheated phase separated $\text{La}_{5/8-y}\text{Pr}_y\text{Ca}_{3/8}\text{MnO}_3$ polycrystalline sample,¹⁸ $\text{La}_{0.77}\text{Ca}_{0.23}\text{MnO}_3$ single crystal,³⁸ and thin (50 nm) $\text{La}_{0.7}\text{Ca}_{0.3}\text{MnO}_3$ film.³⁹ In our experiments, the current flow shifts the MIT to higher temperatures (see Fig. 8). This fact

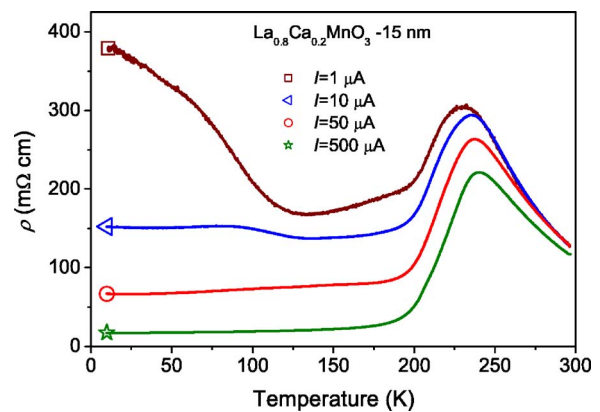


FIG. 8. (Color online) Temperature dependences of resistance recorded at various currents in the high-resistivity state of 15 nm $\text{La}_{0.8}\text{Ca}_{0.2}\text{MnO}_3$ thin film.

enabled us to discard the Joule overheating as a possible source of the observed nonlinear effects.

It is also well known that structural microcracks may develop during thermal cycling of manganite films and lead to tunneling behavior, as was demonstrated in $\text{Nd}_{2/3}\text{Sr}_{1/3}\text{MnO}_3$ films by Satyalakshmi *et al.*⁴⁰ The authors have shown that with respect to uncracked specimens, the cracked films are characterized by much lower temperature of metal-to-insulator transition T_M , 3 orders of magnitude higher resistivity at T_M , and significantly changed form of the temperature dependence of the resistivity at $T > T_M$.⁴⁰ We exclude that similar thermal cycling induced microcracks are responsible for the behavior of our $\text{La}_{0.8}\text{Ca}_{0.2}\text{MnO}_3$ films because none of the above discussed effects showed out in our films during progressed thermal cycling (see Figs. 2, 3, and 8). Although the resistivity of thinner $\text{La}_{0.8}\text{Ca}_{0.2}\text{MnO}_3$ film significantly increases with increasing number of thermal cycles, nevertheless, in a marked contrast to the case of cracked films, the temperature of metal-to-insulator transition remains unchanged. Moreover, microcracks result in irreversible structural changes, which cannot be rejuvenated by a modest thermal treatment at 180 $^\circ\text{C}$, as was observed in our experiments (see Fig. 3).

Comparison of the temperature evolution of resistivity in thinner films (15 nm), thicker films (130 nm), and in single crystals of $\text{La}_{0.8}\text{Ca}_{0.2}\text{MnO}_3$ indicates that despite significant differences in MIT temperature, the transport mechanisms in all samples are apparently the same. We have shown that transport in the paramagnetic state at $T > T_C$ can be described by thermally activated process with single activation energy close to 100 meV. The low-temperature resistivity below T_C exhibits metalliclike behavior ($d\rho/dT > 0$), with the exclusion of the very low temperature range below T_{\min} ($T_{\min} \sim 20$ K for films and ~ 80 K for bulk crystals), where the resistivity upturn is observed. We have determined that within metalliclike conductivity range, the resistivity does not obey the quadratic power dependence on temperature, expected for the pure electron-electron scattering mechanism. A higher value of the power exponent points out to some additional mechanism of low-temperature scattering, most likely to a single magnon scattering.

The Curie temperature in thinner and thicker films is higher than that in single crystals. The difference results most likely from the higher levels of strains in the film samples. The T_C of thinner and more strained 15 nm film is consistently higher than that of the thicker 130 nm film. It appears that in $\text{La}_{0.8}\text{Ca}_{0.2}\text{MnO}_3$ films, the strain effect significantly increases the transfer integral and electron bandwidth, and pushes the sample beyond the percolation threshold, in contrast to $\text{La}_{0.8}\text{Ca}_{0.2}\text{MnO}_3$ single crystals where the ferromagnetic insulating phase dominates at low temperatures.^{4,5,7,8}

The main ingredient for understanding our experimental results is a pronounced phase separation in manganites. In the lowly doped LCMO system, the phase separation results in the coexistence of two FM phases with different orbital orders.^{1,7-9} The analysis of ^{55}Mn and ^{139}La NMR and magnetization data proved that the coexisting phases are characterized by a significantly different magnetic anisotropy and conductivity.^{7,9} In general, the conductivity of a PS system does not depend exclusively on the ratio between volumes occupied by the coexisting phases but depends, in a crucial way, on the distribution sizes and shapes of PS domains. Various external stimuli, such as temperature gradients and applied magnetic or electric field, may influence the topology of the coexisting phases and even cause a change in their volume ratio.⁴¹ Under the influence of an external stimulus, the percolating path of conductive domains became “more insulating” or “more metallic,” leading to differences between transport properties of metastable resistive states in the same sample.

Recent theoretical phase separation models consider phases with different electron densities (electronic phase separation) and/or different structural distortions. Although the evidence for mixed-phase states has been collected in many experimental ways, an unambiguous picture of the topology of a PS system is still not available. The presence of nanoscale chemical inhomogeneities additionally complicates the topology of PS in real samples. The observed phase separation varies from nanometer to micrometer scale length, leading to intricate structures which are too small to be thermodynamic phases in their own right. As a result, a magnetic, electronic, and crystallographic texture appears inside a single complex phase. Moreover, strain interactions can promote mixed-phase textures in the presence of disorder. We believe that dramatic resistivity changes in our samples under progressing thermal cycling and its high sensitivity to applied electric current may be attributed to changing patterns of metallic and insulating regions of the texture within single complex phase.

The electric field and/or current exercises the strongest influence on boundaries between more metallic and more insulating regions, in the areas where the electric field is maximal. Spin polarized electrons accumulating at the boundaries are driven by electric field and/or current and literally pull the boundaries deeper into insulating regions, thus raising the volume occupied by the metallic phase.¹⁴ The shift of boundaries for relatively low currents may be reversible. Alternatively, it was proposed that spin polarized current from FM metallic regions flowing into more insulating regions preserves spin polarization along a certain depth

and thus increases the volume of FM conduction regions.⁴² Recently Viret *et al.*⁴³ considered the effect of electrical current influence on magnetic domain walls (DWs) in conducting ferromagnets with different DW orientations with respect to the current direction. When current is perpendicular to a DW, then the Hall voltage and direct spin transfer will independently induce a pressure capable of moving the DW. When the current direction is not normal to a DW, the electric field in the sample will exercise force on local charges induced on the wall by the Hall effect. Therefore, it is reasonable to suggest that high enough electric current increases volumes of the FM metallic domains and creates a percolative path through the sample, resulting in a strong resistivity decrease at low temperatures.

The comparison of the resistivity between $\text{La}_{0.8}\text{Ca}_{0.2}\text{MnO}_3$ thin films and single crystals in pristine states and in various metastable states shows that the most prominent resistivity changes occur at $T < T_C$, and especially at low temperatures $T \ll T_C$, whereas in the paramagnetic range at $T > T_C$, the changes are relatively small. Such behavior indicates that a change in the topology of FM metallic domains is likely responsible for the pronounced resistivity changes below Curie temperature.

Metastable resistivity can be erased by thermal processing above room temperature. The experimentally determined memory erasing temperature T_E coincides closely with the upper temperature limit for Q_2 structural distortion established from structural measurements.⁹ The temperature T_E can be also identified with the temperature at which the intrinsic energy landscape with hierarchical energy barriers coupled to the strain fields is formed, or with the temperature at which thermal fluctuations start to exceed the pinning energy, such that at $T > T_E$ the domain walls are not effectively pinned by the hierarchical pinning landscape.⁴⁴ The difference between the memory erasing temperature T_E of bulk crystals and that of films may be attributed to a high level of strains in thin-film samples. Clearly, more energy, i.e., higher-temperature treatment, is needed to overcome the elastic energy and to form a new intrinsic energy landscape in thin films.⁴⁴

Sharp resistivity drop observed in the temperature dependence of resistivity of thicker films in the first metastable state shown in Fig. 3 is very similar to the resistivity jumps recently reported for $\text{La}_{5/8-0.3}\text{Pr}_{0.3}\text{Ca}_{3/8}\text{MnO}_3$ manganite thin-film wires.⁴⁵ The jumps were observed in $R(T)$ curves of $\text{La}_{5/8-0.3}\text{Pr}_{0.3}\text{Ca}_{3/8}\text{MnO}_3$ wires of the width reduced down to 1.6 μm . Such jumps were associated with the spatial confinement of the current and reduction of the conduction channels down to a single pathway. It was suggested that when the size of wire decreases to the length scale of a single FM or charge-ordered (CO) domain, the conductivity of a single pathway is temperature driven by CO to FM transition, resulting in a sudden resistivity jump at the transition temperature.⁴⁵ Applying the same mechanism to our case, we find that a transition between competing orbitally ordered more insulating FM phase and orbitally disordered more conductive phase FM phase⁷⁻⁹ within a single pathway of the current may cause a resistivity jump. Progressive shift of the jump temperature to lower temperatures can be attributed to an increase of the volume occupied by less conductive OO

phase under increasing number of thermal cycles. However, in our experiments we did not observe any resistivity jumps in thinner films, where the conduction path is clearly stronger spatially confined, than in the thicker films, where the pronounced jumps appear. This fact proves that the above scenario is not suitable for description of transport properties of $\text{La}_{0.8}\text{Ca}_{0.2}\text{MnO}_3$ thin films and their evolution with thermal cycling and changing electric current.

Our results elucidate the instability of the PS state in thin films, associated with the conversion of a metalliclike FM phase into an insulating FM phase under the perturbation of external or internal stresses induced by the current flow or by the thermal cycling. The PS state instability resembles the one reported previously by us for $\text{La}_{0.8}\text{Ca}_{0.2}\text{MnO}_3$ single crystals. The conducting FM phase in the bulk crystals was found to be much less stable than the insulating phase to such extent that even unperturbed storing of the sample at room temperatures caused a decay of the more conductive orbitally disordered metastable state toward the thermodynamically more stable orbitally ordered insulating FM state.⁵

A significant enhancement of the electric resistivity by dc in $\text{La}_{0.8}\text{Ca}_{0.2}\text{MnO}_3$ epitaxial thin films and its extreme sensitivity to even weak currents resemble the effects observed previously in $\text{La}_{0.8}\text{Ca}_{0.2}\text{MnO}_3$ single crystals. It has to be underlined that dc density required to enforce nonlinear resistivity in thin films is 2–3 orders of magnitude higher than the one causing the same degree of nonlinearity in bulk single crystals.

It has to be emphasized that in a difference to fabricated tunnel junction, one cannot provide an absolute proof for the existence and reality of tunneling processes in phase separated materials. However, the analysis of experimental data provides clear signatures of the domination of tunneling mechanism in the low-temperature conductivity. Indirect evidence is obtained from the nonlinearity of V - I characteristics and their temperature evolution, which are well described by the indirect GM tunneling model (see Figs. 5 and 7). The tunneling conductivity should be associated with intrinsic tunnel junctions arising when percolating metallic paths be-

come separated by insulating regions of less conducting phase. The transport across interrupted metallic paths is dominated by inelastic tunneling of charge carriers across localized states in the barriers separating FM metallic regions. It is interesting to note that as-prepared strained $\text{La}_{0.8}\text{Ca}_{0.2}\text{MnO}_3$ epitaxial thin films exhibit metalliclike behavior below T_C . Nevertheless, in the metastable state their resistivity significantly increases and exhibits low-temperature upturn resembling more that of the single crystals, suggesting that changes in the resistivity and switching into metastable state may be associated with some strain relaxation in the sample. This conclusion is also supported by the transition into higher-resistivity states in bulk samples upon prolonged aging at room temperature. We have tried to verify this hypothesis by means of x-ray measurements of thin films in different resistivity states. First results seem to confirm the hypothesis; nevertheless, the quality of the data does not entitle us to make any decisive conclusions at this stage of the experiments.

IV. CONCLUSIONS

In conclusion, we have studied the effects of thermal cycling and applied current on the transport properties of $\text{La}_{0.8}\text{Ca}_{0.2}\text{MnO}_3$ thin films with thicknesses of 15 and 130 nm deposited on SrTiO_3 substrate. We have performed the resistivity measurements using various protocols. The results reveal metastable states induced by the application of current bias and/or thermal cycling. Metastable states are characterized by the history dependent conductivity, memory effects, and strongly enhanced sensitivity of the resistivity to small current. Metastable resistive state exhibits clear tunneling features associated with development of intrinsic tunneling junctions at low temperatures. The tunneling mechanism dominating charge-transfer mechanism at low temperatures can be regarded as a manifestation of the mixed-phase behavior. The comparison of thin-film data with the results published previously for $\text{La}_{0.8}\text{Ca}_{0.2}\text{MnO}_3$ single crystals shows that transport properties in thin films and bulk crystals are likely controlled by a similar mechanism.

¹E. Dagotto, *Nanoscale Phase Separation and Colossal Magnetoresistance*, Springer Series in Solid State Physics (Springer-Verlag, Berlin, 2003).

²J. B. Goodenough, in *Handbook on the Physics and Chemistry of Rare Earth*, edited by K. A. Gschneidner, Jr., J.-C. G. Bunzli, and V. Pecharsky (Elsevier Science, New York, 2003), Vol. 33.

³P. Levy, F. Parisi, L. Granja, E. Indelicato, and G. Polla, *Phys. Rev. Lett.* **89**, 137001 (2002).

⁴Y. Yuzhelevski, V. Markovich, V. Dikovskiy, E. Rozenberg, G. Gorodetsky, G. Jung, D. A. Shulyatev, and Ya. M. Mukovskii, *Phys. Rev. B* **64**, 224428 (2001); V. Markovich, E. Rozenberg, Y. Yuzhelevski, G. Jung, G. Gorodetsky, D. A. Shulyatev, and Ya. M. Mukovskii, *Appl. Phys. Lett.* **78**, 3499 (2001).

⁵V. Markovich, G. Jung, Y. Yuzhelevski, G. Gorodetsky, A. Szezwczyk, M. Gutowska, D. A. Shulyatev, and Ya. M. Mukovskii, *Phys. Rev. B* **70**, 064414 (2004); V. Markovich, G. Jung, Y.

Yuzhelevski, G. Gorodetsky, and Y. M. Mukovskii, *Eur. Phys. J. B* **48**, 41 (2005).

⁶M. Uehara and S.-W. Cheong, *Europhys. Lett.* **52**, 674 (2000); K. H. Kim, M. Uehara, V. Kiryukhin, and S.-W. Cheong, in *Multi-scale Phase Modulations in Colossal Magnetoresistance Manganites*, edited by C. Tapan (Kluwer Academic, Dordrecht, 2004), p. 131.

⁷G. Papavassiliou, M. Belesi, M. Fardis, and C. Dimitropoulos, *Phys. Rev. Lett.* **87**, 177204 (2001); G. Papavassiliou, M. Pissas, M. Belesi, M. Fardis, J. Dolinsek, C. Dimitropoulos, and J. P. Ansermet, *ibid.* **91**, 147205 (2003); M. Hennion, F. Moussa, P. Lehouelleur, F. Wang, A. Ivanov, Y. M. Mukovskii, and D. Shulyatev, *ibid.* **94**, 057006 (2005).

⁸B. B. Van Aken, O. D. Jurchescu, A. Meetsma, Y. Tomioka, Y. Tokura, and T. T. M. Palstra, *Phys. Rev. Lett.* **90**, 066403 (2003).

- ⁹V. Markovich, E. Rozenberg, A. I. Shames, G. Gorodetsky, I. Fita, K. Suzuki, R. Puzniak, D. A. Shulyatev, and Y. M. Mukovskii, *Phys. Rev. B* **65**, 144402 (2002); V. Markovich, I. Fita, R. Puzniak, M. I. Tsindlekht, A. Wisniewski, and G. Gorodetsky, *ibid.* **66**, 094409 (2002).
- ¹⁰K. Dörr, *J. Phys. D* **39**, R125 (2006).
- ¹¹A. Biswas, M. Rajeswari, R. C. Srivastava, T. Venkatesan, R. L. Greene, Q. Lu, A. L. De Lozanne, and A. J. Millis, *Phys. Rev. B* **63**, 184424 (2001); A. Biswas, M. Rajeswari, R. C. Srivastava, Y. H. Li, T. Venkatesan, R. L. Greene, and A. J. Millis, *ibid.* **61**, 9665 (2000).
- ¹²M. Ziese, H. C. Semmelhack, and K. H. Han, *Phys. Rev. B* **68**, 134444 (2003); M. Ziese, H. C. Semmelhack, K. H. Han, S. P. Sena, and H. J. Blythe, *J. Appl. Phys.* **91**, 9930 (2002).
- ¹³Mandar Paranjape, J. Mitra, A. K. Raychaudhuri, N. K. Todd, N. D. Mathur, and M. G. Blamire, *Phys. Rev. B* **68**, 144409 (2003).
- ¹⁴M. Eblen-Zayas, A. Bhattacharya, N. E. Staley, A. L. Kobrinskii, and A. M. Goldman, *Phys. Rev. Lett.* **94**, 037204 (2005); A. Bhattacharya, M. Elben-Zayas, N. E. Staley, A. L. Kobrinskii, and A. M. Goldman, *Phys. Rev. B* **72**, 132406 (2005).
- ¹⁵J. Gao and F. X. Hu, *Appl. Phys. Lett.* **86**, 092504 (2005); F. X. Hu and J. Gao, *Phys. Rev. B* **69**, 212413 (2004); F. X. Hu, J. Gao, and X. S. Wu, *ibid.* **72**, 064428 (2005).
- ¹⁶R. Shreekala, M. Rajeswari, R. C. Srivastava, K. Ghosh, A. Goyal, V. V. Srinivasu, S. E. Lofland, S. M. Bhagat, M. Downes, R. P. Sharma, S. B. Ogale, R. L. Greene, R. Ramesh, and T. Venkatesan, *Appl. Phys. Lett.* **74**, 1886 (1999).
- ¹⁷W. S. Tan, Q. J. Jia, and J. Gao, *Int. J. Mod. Phys. B* **19**, 2415 (2005).
- ¹⁸J. Sacanell, A. G. Leyva, and P. Levy, *J. Appl. Phys.* **98**, 113708 (2005).
- ¹⁹E. Rozenberg, M. Auslender, I. Felner, and G. Gorodetsky, *J. Appl. Phys.* **88**, 2578 (2000); M. Auslender, A. E. Kar'kin, E. Rozenberg, and G. Gorodetsky, *ibid.* **89**, 6639 (2001).
- ²⁰M. Ziese, *Phys. Rev. B* **68**, 132411 (2003); L. Maritato, C. Adamo, C. Barone, G. M. De Luca, A. Galdi, P. Orgiani, and A. Yu. Petrov, *ibid.* **73**, 094456 (2006).
- ²¹J. M. D. Coey, M. Viret, and S. von Molnar, *Adv. Phys.* **48**, 167 (1999).
- ²²S. Mercone, C. A. Perroni, V. Cataudella, C. Adamo, M. Angeloni, C. Aruta, G. De Filippis, F. Miletto, A. Oropallo, P. Perna, Yu. Petrov, U. Scotti di Uccio, and L. Maritato, *Phys. Rev. B* **71**, 064415 (2005).
- ²³A. Tivary and K. P. Rajeev, *Solid State Commun.* **111**, 33 (1999).
- ²⁴N. Furukawa, *J. Phys. Soc. Jpn.* **69**, 1954 (2000).
- ²⁵M. Ziese, S. Sena, C. Shearwood, H. J. Blythe, M. R. J. Gibbs, and G. A. Gehring, *Phys. Rev. B* **57**, 2963 (1998).
- ²⁶H. Yao, F. X. Hu, and J. Gao, *Thin Solid Films* **495**, 165 (2006).
- ²⁷M. Viret, M. Drouet, J. Nassar, J. P. Contour, C. Fermon, and A. Fert, *Europhys. Lett.* **39**, 545 (1997); J. Z. Sun, *Physica C* **350**, 215 (2001).
- ²⁸A. Asamitsu, Y. Tomioka, H. Kuwahara, and Y. Tokura, *Nature (London)* **388**, 50 (1997).
- ²⁹S. Mercone, A. Wahl, Ch. Simon, and C. Martin, *Phys. Rev. B* **65**, 214428 (2002).
- ³⁰L. I. Glazman and K. A. Matveev, *Sov. Phys. JETP* **67**, 1276 (1988) [*Zh. Eksp. Teor. Fiz.* **94**, 332 (1988)].
- ³¹V. Markovich, E. S. Vlahov, Y. Yuzhelevskii, B. Blagoev, K. A. Nenkov, and G. Gorodetsky, *Phys. Rev. B* **72**, 134414 (2005).
- ³²V. Markovich, G. Jung, M. Belogolovskii, Y. Yuzhelevskii, G. Gorodetsky, and Ya. M. Mukovskii, *Eur. Phys. J. B* **50**, 587 (2006).
- ³³G. Garbarino, M. Monteverde, C. Acha, P. Levy, M. Quintero, T. Y. Koo, and S.-W. Cheong, *Physica B* **354**, 16 (2004).
- ³⁴P. Padhan, W. Prellier, Ch. Simon, and R. C. Budhani, *Phys. Rev. B* **70**, 134403 (2004).
- ³⁵A. N. Lavrov, I. Tsukada, and Y. Ando, *Phys. Rev. B* **68**, 094506 (2003).
- ³⁶S. Mercone, R. Frésard, V. Caignaert, C. Martin, D. Saurel, C. Simon, G. André, P. Monod, and F. Fauth, *J. Appl. Phys.* **98**, 023911 (2005).
- ³⁷B. Fisher, J. Genossar, K. B. Chashka, L. Patlagan, and G. M. Reisner, *Appl. Phys. Lett.* **88**, 152103 (2006).
- ³⁸L. Sudheendra and C. N. R. Rao, *J. Appl. Phys.* **94**, 2767 (2003).
- ³⁹A. Palanisami, M. B. Weissman, and N. D. Mathur, *Phys. Rev. B* **71**, 094419 (2005).
- ⁴⁰K. M. Satyalakshmi, B. Fisher, L. Patlagan, G. Koren, E. Sheriff, R. Prozorov, and Y. Yeshurun, *Appl. Phys. Lett.* **73**, 402 (1998).
- ⁴¹D. Khomskii and L. Khomskii, *Phys. Rev. B* **67**, 052406 (2003).
- ⁴²Y. G. Zhao, Y. H. Wang, G. M. Zhang, B. Zhang, X. P. Zhang, C. X. Yang, P. L. Lang, M. H. Zhu, and P. C. Guan, *Appl. Phys. Lett.* **86**, 122502 (2005).
- ⁴³M. Viret, A. Vanhaverbeke, F. Ott, and J.-F. Jacquinet, *Phys. Rev. B* **72**, 140403(R) (2005).
- ⁴⁴K. H. Ahn, T. Lookman, and A. R. Bishop, *Nature (London)* **428**, 401 (2004).
- ⁴⁵Hong-Ying Zhai, J. X. Ma, D. T. Gillaspie, X. G. Zhang, T. Z. Ward, E. W. Plummer, and J. Shen, *Phys. Rev. Lett.* **97**, 167201 (2006).